Development 138, 5415-5427 (2011) doi:10.1242/dev.069831

Rho GTPase controls *Drosophila* salivary gland lumen size through regulation of the actin cytoskeleton and Moesin

Na Xu[1,2], Gaiana Bagumian[2], Michael Galiano[2] and Monn Monn Myat[2,*]

SUMMARY

Generation and maintenance of proper lumen size is important for tubular organ function. We report on a novel role for the *Drosophila* Rho1 GTPase in control of salivary gland lumen size through regulation of cell rearrangement, apical domain elongation and cell shape change. We show that Rho1 controls cell rearrangement and apical domain elongation by promoting actin polymerization and regulating F-actin distribution at the apical and basolateral membranes through Rho kinase. Loss of *Rho1* resulted in reduction of F-actin at the basolateral membrane and enrichment of apical F-actin, the latter accompanied by enrichment of apical phosphorylated Moesin. Reducing cofilin levels in *Rho1* mutant salivary gland cells restored proper distribution of F-actin and phosphorylated Moesin and rescued the cell rearrangement and apical domain elongation defects of *Rho1* mutant glands. In support of a role for Rho1-dependent actin polymerization in regulation of gland lumen size, loss of profilin phenocopied the *Rho1* lumen size defects to a large extent. We also show that Ribbon, a BTB domain-containing transcription factor functions with Rho1 in limiting apical phosphorylated Moesin for apical domain elongation. Our studies reveal a novel mechanism for controlling salivary gland lumen size, namely through Rho1-dependent actin polymerization and distribution and downregulation of apical phosphorylated Moesin.

KEY WORDS: *Drosophila*, Rho GTPase, Actin, Lumen, Salivary gland, Tube

INTRODUCTION

Epithelial tubes are the structural and functional components of many essential organs, such as the respiratory, circulatory and secretory organs. Tubular organs serve important physiological roles, including delivery of gases, nutrients and hormones, and removal of waste. Tube morphogenesis is a highly regulated process that requires dynamic cell shape changes, cell migration and cell rearrangements, as well as remodeling of cell adhesion junctions and select membrane domains (Andrew and Ewald, 2010; Jung et al., 2005; Lubarsky and Krasnow, 2003; Martin-Belmonte and Mostov, 2008). All tubular organs contain a lumen the size and shape of which is essential for organ function. Failure to achieve and/or maintain proper lumen size and shape can lead to pathological conditions. For example, polycystic kidney disease is characterized by lumen expansion whereas stenoses are characterized by abnormal narrowing of blood vessels.

The Rho family of small GTPases, which includes Rac, Cdc42 and Rho, are required for multiple cellular events, such as cell motility, proliferation and gene transcription. A crucial role for Rac and Cdc42 in lumen morphogenesis is well documented (Davis et al., 2007; Jaffe et al., 2008; Martin-Belmonte et al., 2007). Mammalian Cdc42 regulates microlumen formation and maintains cell polarity during pancreatic tube morphogenesis (Kesavan et al., 2009). In three-dimensional Caco-2 cell cultures, Cdc42 prevents multiple lumen formation by orienting cell divisions and directing apical membrane growth (Jaffe et al., 2008). We recently showed that in the *Drosophila* salivary gland, Cdc42 and the p21 activated kinase (Pak) 1 regulate gland lumen size (Pirraglia et al., 2010). In contrast to Cdc42 and Rac GTPases, the role of Rho in tube and lumen morphogenesis is poorly understood.

The only *Drosophila* Rho GTPase, Rho1, is required for invagination of the salivary gland and the posterior spiracles (Simoes et al., 2006; Xu et al., 2008). After invaginating from the ventral surface of the embryo, salivary gland cells migrate collectively as an intact tube, with the distal tip cells elongating and extending protrusions in the direction of migration (Bradley et al., 2003), and the proximal end cells changing shape from columnar to cuboidal (Xu et al., 2008). When the distal gland cells contact the overlying circular visceral mesoderm (CVM), the entire gland turns and migrates posteriorly (Bradley et al., 2003; Vining et al., 2005). Contact between the distal gland cells and the CVM is mediated through the integrin adhesion receptors; loss of the βPS or the αPS2 integrin subunits results in glands that fail to turn and migrate posteriorly (Bradley et al., 2003). We previously showed that Rho1 controls salivary gland invagination and migration by regulating cell polarity and Rok-mediated cell contraction and that Rho1 activity is required in the gland cells as well as in the CVM (Xu et al., 2008).

The *Drosophila* embryonic salivary gland is a well-established model system for investigating lumen size control in a tubular organ. After salivary gland cells invaginate, they undergo a phase of robust apical surface membrane growth (Myat and Andrew, 2002) and the apical domain size of individual cells decreases and elongates to become anisotropic along the longest axis of the lumen (Pirraglia et al., 2010). Apical membrane growth is limited by the basic helix-loop-helix (bHLH) transcriptional repressor Hairy and its regulation of Huckebein (Hkb), an Sp1/Egr-like transcription factor, and by target genes *klarsicht* (*klar*), which encodes a KASH-domain-containing regulator of organelle and nuclear transport (Fischer-Vize and Mosley, 1994; Fischer et al., 2004; Guo

[1]BCMB Program of Weill Graduate School of Medical Sciences at Cornell University, 1300 York Avenue, New York, NY 10065, USA. [2]Department of Cell and Developmental Biology, Weill Medical College of Cornell University, 1300 York Avenue, New York, NY 10065, USA.

*Author for correspondence (mmm2005@med.cornell.edu)

Accepted 11 October 2011

et al., 2005; Mosley-Bishop et al., 1999) and *crumbs* (*crb*), which encodes an apical membrane protein that is necessary for the establishment and maintenance of apical-basal polarity (Myat and Andrew, 2002; Tepass and Knust, 1993; Tepass et al., 1990). Apical membrane remodeling in salivary gland cells is also regulated by Ribbon (Rib), a Broad Tramtrack Bric-a-brac (BTB) domain transcription factor (Bradley and Andrew, 2001; Shim et al., 2001), which promotes Crb expression and limits apical activity of the ERM protein Moesin (Kerman et al., 2008). Based on mathematical modeling, it is thought that salivary gland lumens of *rib* mutant embryos fail to elongate because of increased apical surface stiffness and viscosity (Cheshire et al., 2008). We recently showed that apical domain elongation is regulated by Pak1 through differential localization of E-cadherin (E-cad; Shotgun – FlyBase) at the adherens junctions and at the basolateral membrane (Pirraglia et al., 2010). Here, we provide the first evidence that Rho1 controls lumen size in the *Drosophila* embryonic salivary gland through regulation of the actin cytoskeleton and Moesin.

MATERIALS AND METHODS

Drosophila strains and genetics

Canton-S flies were used as wild-type controls. The following fly lines were obtained from the Bloomington Stock Center and are described in FlyBase (http://flybase.bio.indiana.edu/): $Rho1^{K02107b}$ ($Rho1^{K}$), $Rho1^{1B}$, $Rho1^{E3.10}$, $Rho1^{72O}$ $Rho1^{72F}$, *armadillo* (*arm*)-GAL4, UAS-Rok^{CA}, rib^{1}, rok^{2}, $chic^{221}$, tsr^{k05366}, UAS-$Rab5^{S43N}$ (UAS-$Rab5^{DN}$), UAS-Shi^{K44A} (UAS-Shi^{DN}) and UAS-Dicer. UAS-*Rok*-RNAi was obtained from Vienna *Drosophila* RNAi Center (http://stockcenter.vdrc.at/). UAS-Moe^{T559A} and UAS-Moe^{T559D} were gifts from R. Fehon (University of Chicago, Chicago, USA). UAS Rib^{WT} and UAS $Rho1^{WT}$ were gifts from D. Andrew (Johns Hopkins University School of Medicine, MD, USA) and N. Harden (Simon Fraser University, Burnaby, Canada), respectively. UAS E-cadherin-GFP was obtained from H. Oda (JT Biohistory Research Hall, Osaka, Japan). *fork head* (*fkh*-GAL4) was used to drive salivary gland-specific expression (Henderson and Andrew, 2000). UAS-*Rok*-RNAi expression was driven with *arm*-GAL4; *fkh*-GAL4. *Twist*-GAL4 was a gift from M. Baylies (Memorial Sloan-Kettering Cancer Center, NY, USA).

Antibody staining of embryos

Embryo fixation and staining were performed as previously described (Reuter et al., 1990). F-actin was stained with Phalloidin (1:20; Invitrogen) as previously described (Jani and Schöck, 2007). The following antisera were used at the indicated dilutions: rat or rabbit (a gift from D. Andrew) dCREB-A antiserum at 1:10,000 for diaminobenzidine (DAB) staining and 1:250 for fluorescence; rabbit DaPKC antiserum (Santa Cruz Biotechnology, Santa Cruz, CA, USA) at 1:500; Neurotactin antiserum [Developmental Studies Hybridoma Bank (DSHB), Iowa City, IA, USA] at 1:10; mouse α-spectrin antiserum (DSHB) at 1:10; rabbit phospho-Moe antiserum (Cell Signaling Technology, Danvers, MA, USA) at 1:100; mouse β-galactosidase (β-gal) antiserum (Promega; Madison, WI, USA) at 1:10,000 for DAB staining and 1:500 for fluorescence; rat Rib antiserum (a gift from D. Andrew) at 1:50; rabbit anti-Avalanche antiserum at 1:1000 (a gift from H. Kramer, UT Southwestern Medical Center, Dallas, TX, USA), and rat E-cad and α-catenin antisera (DSHB) at 1:20. Appropriate biotinylated (Jackson ImmunoResearch Laboratories, Westgrove, PA, USA) and AlexaFluor488-, AlexaFluor647- or Rhodamine- (Molecular Probes, Eugene, OR, USA) conjugated secondary antibodies were used at a dilution of 1:500. Whole-mount (DAB stained) embryos were mounted in methyl salicylate (Sigma, St Louis, MO, USA) before visualization on a Zeiss Axioplan 2 microscope with Axiovision Rel 4.8 software (Carl Zeiss, Thornwood, NY, USA). Fluorescently labeled embryos were mounted with Aqua Polymount (Polysciences, Warrington, PA, USA). Fluorescent images of sections (0.5 or 1 μm thick) were acquired on a Zeiss Axioplan microscope (Carl Zeiss) equipped for laser scanning confocal microscopy at the Rockefeller University Bio-imaging Resources Center (New York, NY, USA) and the Weill Cornell Optical Core Facility.

Morphometric analyses

All measurements of lumen length, lumen width, apical domain elongation ratio, apical-basal axis length and number of nuclei were performed with LSM 510 Image Browser software (Carl Zeiss). Lumen length measurements were based on E-cad immunofluorescence staining of stage 13 embryos, from the proximal tip to the distal tip of gland lumens. Lumen width was measured in the middle of the proximal one third of the gland, approximately eight cells away from the proximal end of the gland (supplementary material Fig. S1). Apical domain elongation ratio of an individual gland cell was measured according to E-cad immunofluorescence staining of stage 12 embryos. Elongation ratio represents the ratio of a single measurement of the longest length of the apical domain oriented along the proximal-distal axis to a single measurement of the longest length of the apical domain along the dorsal-ventral axis (Pirraglia et al., 2010). Measurements of apical domain elongation ratio were performed with the eight most proximal cells in each gland. Apical-basal axis length was visualized using Neurotactin and DaPKC staining of stage 12 embryos, and was measured from the basal to the apical membrane of the four most proximal cells at the anterior side of each gland. The number of nuclei surrounding the lumen was counted based on orthogonal views of E-cad- and dCREB-A-stained stage 12 embryos, in the proximal one third of the gland, approximately eight cells away from the proximal end. Statistical analysis was conducted using Microsoft Excel (Microsoft, Redmond, WA, USA) and STATA software (Statacorp, TX, USA).

Measurement of embryo size

To measure embryo size, stage 12 $Rho1^{1B}$ heterozygous and homozygous embryos were first stained for Crumbs to label the ectoderm and β-galactosidase to distinguish heterozygous from homozygous embryos. A single measurement of embryo length along the anterior-posterior axis and a single measurement of embryo height along the dorsal-ventral axis were made and the ratio of embryo length to embryo height was calculated. Measurements were made using Zeiss Axiovision Rel 4.8 software (Carl Zeiss).

Quantification of fluorescence intensity

For quantification of total fluorescence intensity, stage 12 $Rho1^{1B}$ or rib^{1} homozygous and heterozygous embryos were double-stained for E-cad and α-spectrin or α-catenin and α-spectrin. Three sets of *z* series, each consisting of 1 μm-thick optical sections, were acquired by LSM confocal microscopy and the projected image of each *z* series was analyzed using ImageJ software (NIH). Identical areas measuring 3 μm in width and 3 μm in length were selected in the four proximal-most gland cells and the average fluorescence intensity (in pixels) of E-cad was normalized against the average fluorescence intensity of α-spectrin within the same area.

For quantification of the ratio of apical to basolateral F-actin or p-Moe, stage 12 WT, $Rho1^{1B}$, $Rho1^{E3.10}$, rib^{1}, Moe^{T559D}, $Rho1^{1B}Rib^{WT}$, $Rho1^{1B}Moe^{T559A}$, $chic^{221}$, tsr^{K}, $tsr^{K}Rho1^{1B}$ or *Rok-RNAi* expressing embryos were stained with F-actin and/or p-Moe. A single *z* series acquired by LSM confocal microscopy was selected and analyzed by ImageJ software. Identical areas measuring 2.09 μm in width and 2.09 μm in length were selected in the middle of the apical or basolateral domain of the four proximal-most salivary gland cells. The ratio of the average fluorescence (in pixels) intensity of apical F-actin or p-Moe to that of basolateral F-actin or p-Moe was then calculated.

RESULTS

Rho1 controls salivary gland lumen size

We previously showed that Rho1 is required in salivary gland cells and in the surrounding mesoderm to regulate invagination and migration of the gland (Xu et al., 2008). In $Rho1^{1B}$ mutant embryos, salivary gland cells invaginated and formed a tube with a central lumen but failed to migrate posteriorly, whereas in $Rho1^{K}$ mutant embryos, most gland cells did not invaginate and did not form a tube (Xu et al., 2008) (Table 1). $Rho1^{K}$ is a loss-

Table 1. Rho1 mutant alleles and their salivary gland phenotypes

Alleles	Nature of alleles	Salivary gland phenotypes
$Rho1^{K}$	P element insertion in the first intron (Magie et al., 1999)	Invagination and cell polarity defects (Xu et al., 2008)
$Rho1^{72O}$	P element insertion, lack of translation start codon (Strutt et al., 1997)	Invagination defects (data not shown)
$Rho1^{1B}$	Premature stop codon removing 2/3 coding sequence from C terminus (Magie and Parkhurst, 2005)	Migration defects and abnormal lumen size (Xu et al., 2008) (this study)
$Rho1^{E3.10}$	Missense mutation in the CAAX box, reducing membrane-bound Rho1 (Halsell et al., 2000)	Migration defects and abnormal lumen size (this study)
$Rho1^{72F}$	P element insertion, lack of translation start codon (Strutt et al., 1997)	Migration defects and abnormal lumen size (Xu et al., 2008) (this study)
$Rho1^{N19}$	Dominant negative (Strutt et al., 1997)	Invagination, migration and polarity defects (Xu et al., 2008)
$Rho1^{V12}$	Constitutively active (Rangarajan et al., 1999)	Salivary gland cells invaginate simultaneously and form multiple lumens (Xu et al., 2008)

of-function allele with a P element insertion in the first intron (Magie et al., 1999). $Rho1^{1B}$ is a loss-of-function allele in which the coding region C-terminal to amino acid 52 is removed by an imprecise P-element excision (Magie and Parkhurst, 2005). No Rho1 protein is detected by immunohistochemistry in $Rho1^{1B}$ homozygous embryos (Magie and Parkhurst, 2005). The severity of the $Rho1^{K}$ allele is comparable to that of glands expressing dominant-negative Rho1 (Table 1). To determine a role for Rho1 in control of salivary gland lumen size, we analyzed three different alleles of Rho1, $Rho1^{1B}$, $Rho1^{E3.10}$ and $Rho1^{72F}$ (Table 1). The $Rho1^{E3.10}$ allele is a loss-of-function allele in which the cysteine residue at position 189 is changed to a tyrosine residue (Halsell et al., 2000) and the $Rho1^{72F}$ allele is a loss-of-function allele lacking part of the coding region including the translation start site (Strutt et al., 1997). Because the cysteine at position189 is the first residue in the CAAX box and is the site of post-translational prenylation, the $Rho1^{E3.10}$ mutant protein is unlikely to get prenylated and is likely to fail to localize to the plasma membrane to be activated. In embryos homozygous for $Rho1^{1B}$, $Rho1^{E3.10}$ or $Rho1^{72F}$, all gland cells invaginated and formed a tubular organ (data not shown), allowing us to analyze Rho1 function in lumen size control.

In wild-type glands, the lumen diameter in the proximal region of the gland gradually decreased between embryonic stages 11 and 12 as the gland turned and migrated posteriorly, whereas lumen diameter in the medial and distal regions did not change (Pirraglia et al., 2010) (supplementary material Fig. S1). In $Rho1^{1B}$ mutant embryos, lumen length was 60% of that of heterozygous siblings and lumen width in the proximal region was approximately twice that of heterozygous siblings (Fig. 1A-F). Embryos homozygous

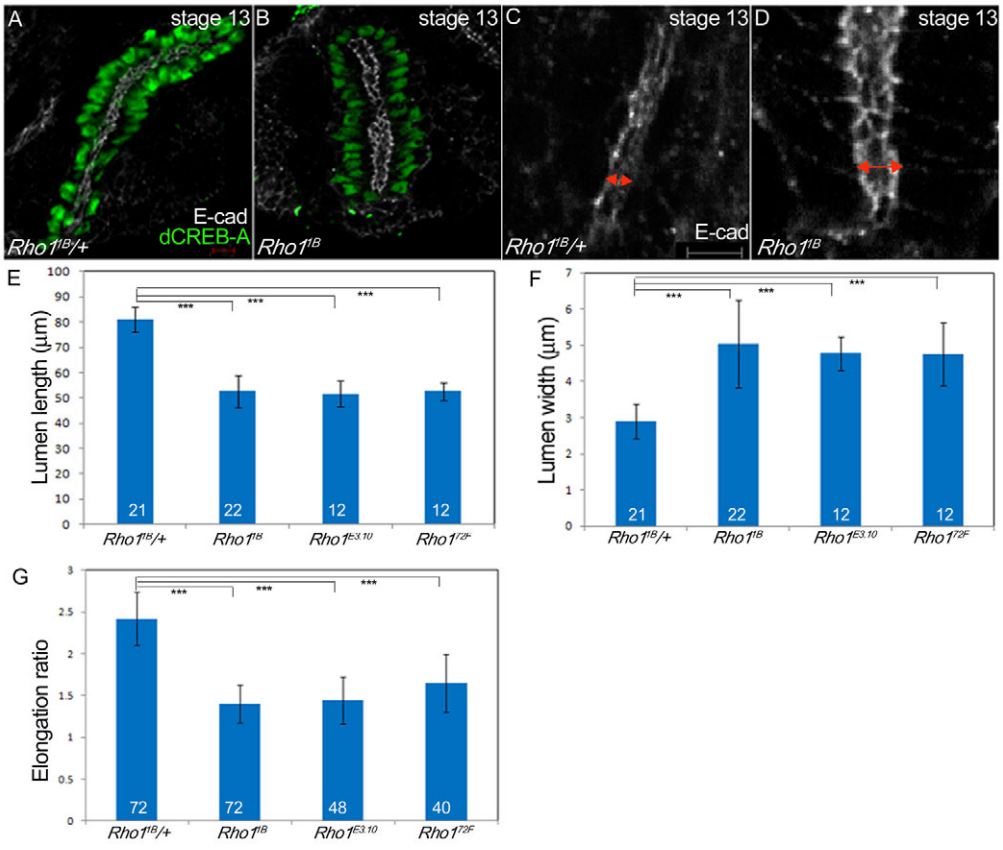

Fig. 1. Rho1 controls salivary gland lumen size.
(**A-D**) *Drosophila* embryos stained for E-cad (white) to label the lumen and dCREB-A (green) to label salivary gland nuclei. The gland lumen of $Rho1^{1B}$ heterozygous embryos (A,C) is elongated (A, white) and is of a distinct width (C, red arrow), whereas that of homozygous siblings (B,D) is shortened (B, white) and widened (D, red arrow). Scale bars: 5 μm in A; 2 μm in C. (**E-G**) Graphs depicting measurements of lumen length (E), lumen width (F) and apical domain elongation ratio (G) in $Rho1^{1B}$ heterozygous and homozygous embryos and $Rho1^{E3.10}$ and $Rho1^{72F}$ homozygous embryos. ***P<0.001. Numbers on bars represent the number of glands (E,F) or gland cells (G) measured. Error bars represent s.d.

for *Rho1*$^{E3.10}$ or *Rho1*^{72F} showed defects in gland lumen size of the same severity as those in *Rho1*^{1B} mutant embryos (Fig. 1E,F). To confirm that lumen size defects in *Rho1* mutant embryos were not a consequence of changes in embryo size, we measured embryo length and height in *Rho1*^{1B} heterozygous and homozygous embryos. These measurements showed that embryo size was comparable in *Rho1*^{1B} heterozygous and homozygous embryos, demonstrating that salivary gland lumen size did not correlate with embryo size (data not shown).

Changes in salivary gland lumen length and width are normally accompanied by gradual elongation of the apical domain along the proximal-distal (Pr-Di) axis of the gland between stage 11, when the cells are internalized, and stage 12, when they migrate collectively (Pirraglia et al., 2010). Failure to elongate the apical domain can result in gland lumen size defects (Pirraglia et al., 2010). Therefore, we analyzed the extent of apical domain elongation in *Rho1*^{1B} homozygous gland cells compared with those of heterozygous siblings, and found that apical domains of *Rho1*^{1B} mutant gland cells did not elongate in the Pr-Di axis to the same extent as did apical domains of heterozygous siblings (Fig. 1G). We limited our analysis to the proximal gland cells, which showed the greatest reduction in lumen width (Pirraglia et al., 2010) and where Rho1 activity is predominantly required (Xu et al., 2008). Embryos homozygous for *Rho1*$^{E3.10}$ or *Rho1*^{72F} also showed defects in apical domain elongation of the same severity as those in *Rho1*^{1B} homozygous embryos (Fig. 1G).

One mechanism for controlling apical domain elongation is through differential localization of E-cadherin (E-cad) at the adherens junctions (AJs) and at the basolateral membrane in a manner dependent on Pak1- and Rab5-mediated endocytosis (Pirraglia et al., 2010). In *Pak1* mutant embryos, apical domains were expanded and failed to elongate in the Pr-Di axis concomitant with enhanced localization of E-cad at the AJs and reduced localization at the basolateral membrane (Pirraglia et al., 2010). In contrast to *Pak1* mutant embryos, in *Rho1*^{1B} homozygous embryos, E-cad continued to be localized to the basolateral membrane and levels of E-cad at the AJs and at the basolateral membrane were similar in *Rho1*^{1B} homozygous and heterozygous gland cells (supplementary material Fig. S2). Similar to E-cad, localization of α-Catenin, another component of the AJs, was not affected in *Rho1*^{1B} mutant gland cells (data not shown). Moreover, expression of wild-type E-cad, encoded by *shotgun* (*shg*), specifically in gland cells of *Rho1*^{1B} mutant embryos, did not enhance or suppress the lumen size defects, or defects in cell shape change and apical domain elongation, and only slightly alleviated the cell rearrangement defects of *Rho1*^{1B} homozygous embryos (supplementary material Fig. S3). During gland invagination, Rho1 is required to maintain E-cad at the AJs; in *Rho1*^{K} homozygous embryos where salivary gland cells did not maintain apical polarity (Xu et al., 2008), E-cad was lost from the apical-lateral membrane (supplementary material Fig. S4). Loss of E-cad in *Rho1*^{K} mutant gland cells is possibly a secondary consequence of loss of apical polarity proteins, such as Crb, Stardust and atypical PKC (Xu et al., 2008). Thus, our analysis of *Rho1* mutant embryos demonstrates that Rho1 regulates salivary gland lumen size without affecting levels of E-cad at the AJs or at the basolateral membrane.

Rho1-dependent cell rearrangement is required for salivary gland lumen size control

Rho-mediated signaling is known to control the cell rearrangements that drive elongation of the vertebrate gut tube (Reed et al., 2009). Thus, we hypothesized that Rho1 controls salivary gland lumen size, at least in part, by regulating cell rearrangement. To test this hypothesis, we first determined whether cell rearrangement normally occurred during elongation and narrowing of the gland lumen. We measured the extent of cell rearrangement in the proximal gland cells by counting the number of nuclei that surrounded the central lumen. In stage 11 wild-type glands, between ten and 12 cells (nuclei) surrounded the lumen in the proximal region of the gland (Fig. 2A,E). As the gland lumen elongated and narrowed proximally between stages 11 and 13, we observed a decrease in the number of nuclei surrounding the lumen, such that by stage 13, approximately half the number of nuclei surrounded the lumen compared with stage 11 (Fig. 2A-C,E). In contrast to wild-type glands, proximal gland cells of *Rho1*^{1B} mutant embryos failed to rearrange; in stage 12 *Rho1*^{1B} mutant glands, the

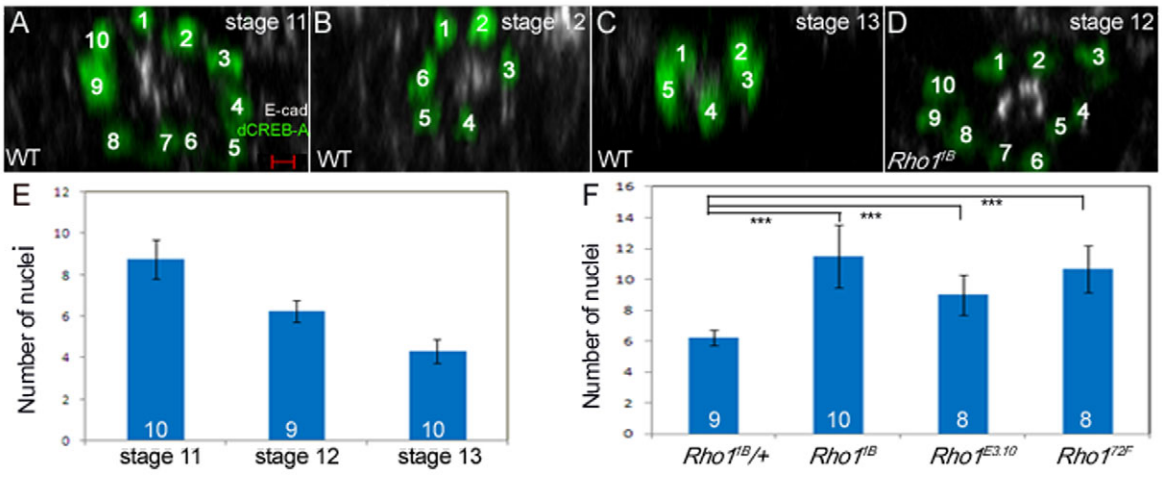

Fig. 2. Rho1-mediated cell rearrangement is important for salivary gland lumen size control. (**A-D**) Orthogonal views of *Drosophila* embryos stained for E-cad (white) to label the lumen and dCREB-A (green). Cells (numbered) in the proximal region of wild-type glands rearrange to form a narrow tube (A-C), whereas cells of *Rho1*^{1B} mutant glands failed to rearrange and instead formed a wide tube (D). Scale bar: 3 μm. (**E**,**F**) Graphs depicting the number of nuclei surrounding the proximal gland lumen of wild-type embryos between stages 11 and 13 (E) and glands of *Rho1*^{1B} heterozygous and homozygous embryos and *Rho1*$^{E3.10}$ and *Rho1*^{72F} homozygous embryos at stage 12 (F). ***P<0.001. Numbers on bars represent the number of glands measured. Error bars represent s.d.

number of nuclei surrounding the gland was approximately twofold greater than that of heterozygous siblings (Fig. 2D,F). Embryos homozygous for *Rho1*$^{E3.10}$ or *Rho1*^{72F} also showed defects in cell rearrangement (Fig. 2F). Thus, Rho1 function is required for the cell rearrangements that normally occur during salivary gland lumen elongation and narrowing.

Rho1 controls salivary gland lumen size through Rho kinase

We previously showed that Rho kinase (Rok), a key downstream effector of Rho GTPase, is required for gland migration, in particular for the proximal gland cells to flatten and change shape from columnar to cuboidal (Xu et al., 2008), which is quantified here as changes in apical-basal axis length. To test whether Rok was also required for the Rho1-dependent control of gland lumen size, we analyzed gland lumen size in embryos in which Rok function was specifically inhibited in the gland using RNAi knockdown. To achieve maximal knockdown of Rok, we co-expressed *Rok-RNAi* and *Dicer* with *fork head* (*fkh*)-GAL4 and *armadillo*-GAL4. Lumens of *Rok-RNAi*-expressing glands were widened like those of *Rho1*^{1B} mutant glands; however, lumen length in *Rok-RNAi*-expressing glands was only mildly affected (Fig. 3A,B). *Rok-RNAi*-expressing glands also had defects in cell shape change, apical domain elongation and cell rearrangement (Fig. 3C-E). Although we observed mild lumen length defects in *Rok-RNAi*-expressing glands, lumen length was shorter in glands of embryos homozygous for a loss-of-function allele of *Rok*, *rok*^{2} (Fig. 3A). *rok*^{2} mutant glands also showed defects in lumen width, cell shape change, apical domain elongation and cell rearrangement (Fig. 3B-E). Gland-specific expression of constitutively active Rok (Rok^{CA}) in *Rho1*^{1B} mutant glands was sufficient to partially restore lumen length and completely restore lumen width in *Rho1*^{1B} mutant glands (Fig. 3A,B). Expression of *Rok*^{CA} allowed *Rho1*^{1B} mutant gland cells to change shape, to rearrange and for the apical domains to elongate (Fig. 3C-E). These data demonstrate that Rok mediates Rho1-dependent cell shape change, apical domain elongation and cell rearrangement, all processes that collectively determine salivary gland lumen size.

Rho1 functions cell-autonomously to regulate apical domain elongation and cell rearrangement

We previously showed that Rho1 activity is required in the salivary gland, predominantly in the proximal gland cells, and surrounding mesoderm for gland migration (Xu et al., 2008). To

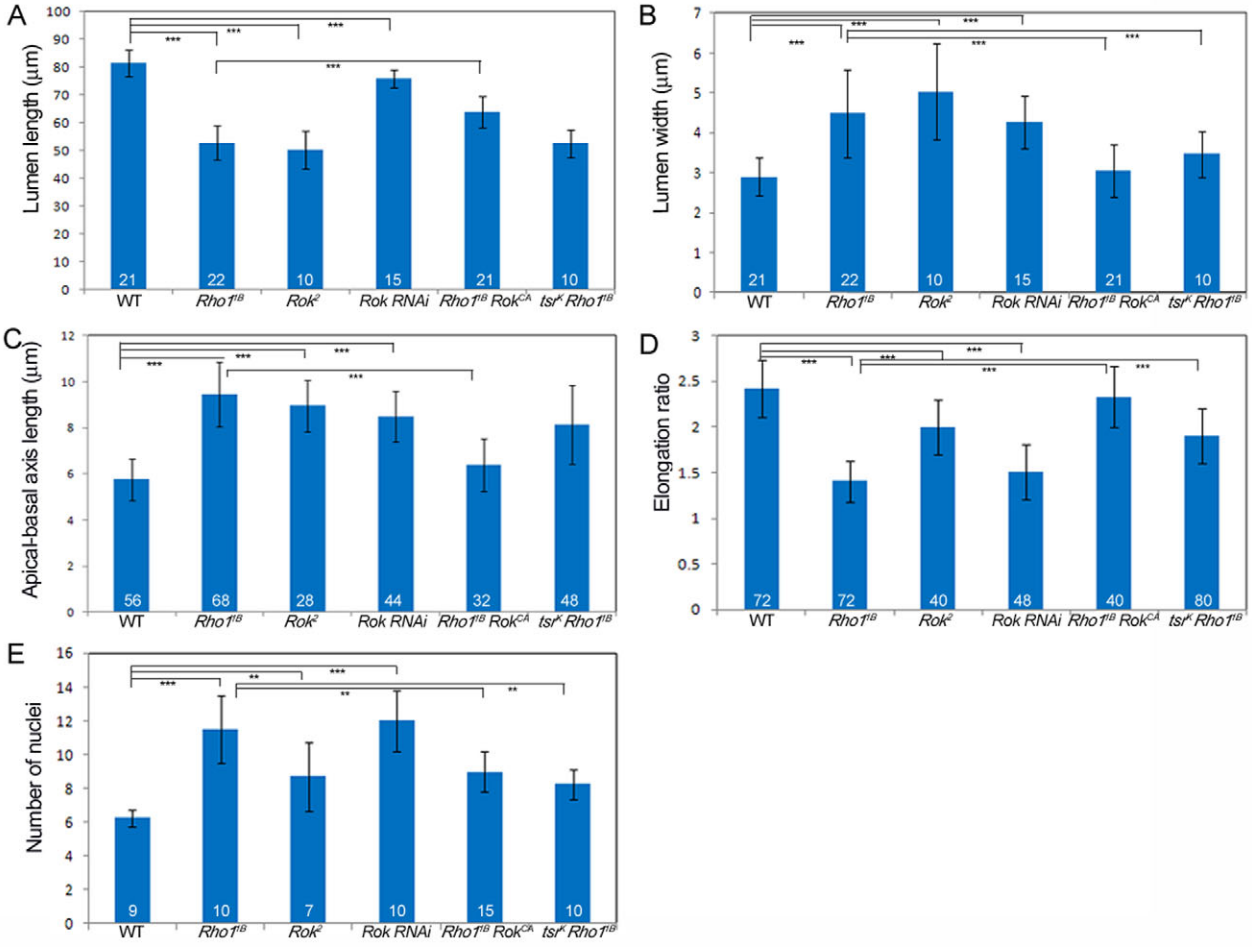

Fig. 3. Rho1 regulates salivary gland lumen size through Rok. (**A-E**) Graphs depicting measurements of lumen length (A) and width (B), apical-basal axis length (C), apical domain elongation ratio (D) and number of nuclei surrounding the salivary gland lumen (E) of wild-type (WT) *Drosophila* embryos, *Rho1*^{1B} homozygous embryos, *rok*^{2} homozygous embryos, wild-type embryos expressing *Rok RNAi* in the gland, *Rho1*^{1B} homozygous embryos expressing *Rok*^{CA} in the gland and *tsr*^{K}*Rho1*^{1B} double mutant embryos. $^{**}P<0.01$, $^{***}P<0.001$. Numbers on bars represent the number of glands (A,B,E) or the number of cells (C,D) measured. Error bars represent s.d.

test whether Rho1 function is required in gland cells for lumen size control, we expressed wild-type *Rho1* ($Rho1^{WT}$) in all gland cells with *fkh*-GAL4, in just the proximal gland cells with *engrailed* (*en*)-GAL4 or in the surrounding mesoderm with *twist* (*twi*)-Gal4. Expression of $Rho1^{WT}$ in either the salivary gland or surrounding mesoderm of $Rho1^{1B}$ homozygous embryos had no effect on gland lumen length or width (supplementary material Fig. S5A,B). However, expression of $Rho1^{WT}$ in all gland cells or just the proximal gland cells of $Rho1^{1B}$ homozygous embryos led to a partial but significant rescue of the apical domain elongation and cell rearrangement defects (supplementary material Fig. S5D,E). By contrast, expression of $Rho1^{WT}$ in the mesoderm only slightly alleviated the apical elongation defect and had no effect on the cell rearrangement defect of $Rho1^{1B}$ mutant embryos (supplementary material Fig. S5D,E). Expression of $Rho1^{WT}$ in either the gland or the mesoderm had only a mild effect on cell shape change (supplementary material Fig. S5C). From these data we conclude that Rho1 functions predominantly in the proximal salivary gland cells to control apical domain elongation and cell rearrangement.

Rho1 is required for actin polymerization and distribution in salivary gland cells

Rho family GTPases are known to regulate the actin cytoskeleton, with mammalian RhoA being most directly linked to the formation of stress fibers (Ridley and Hall, 1992). Therefore, we tested whether the lumen size defects of $Rho1^{1B}$ mutant glands could be due to defects in the actin cytoskeleton by analyzing the distribution of cortical F-actin at the apical and basolateral membranes. We quantified F-actin distribution by measuring the ratio of F-actin at the apical membrane to that at the basolateral membrane. In proximal gland cells of $Rho1^{1B}$ heterozygous embryos, the apical membrane was slightly more enriched with F-actin compared with the basolateral membrane (Fig. 4A). In $Rho1^{1B}$ mutant gland cells, the apical membrane was highly enriched with F-actin whereas F-actin was severely reduced at the basolateral membrane (Fig. 4B). Moreover, the apical to basolateral (A/Bl) F-actin ratio of $Rho1^{1B}$ mutant gland cells was significantly higher than that of wild-type gland cells (Fig. 4K). $Rho1^{E3.10}$ mutant glands and Rok-RNAi-expressing glands also had reduced basolateral F-actin and enriched apical F-actin (Fig. 4C,K; data not

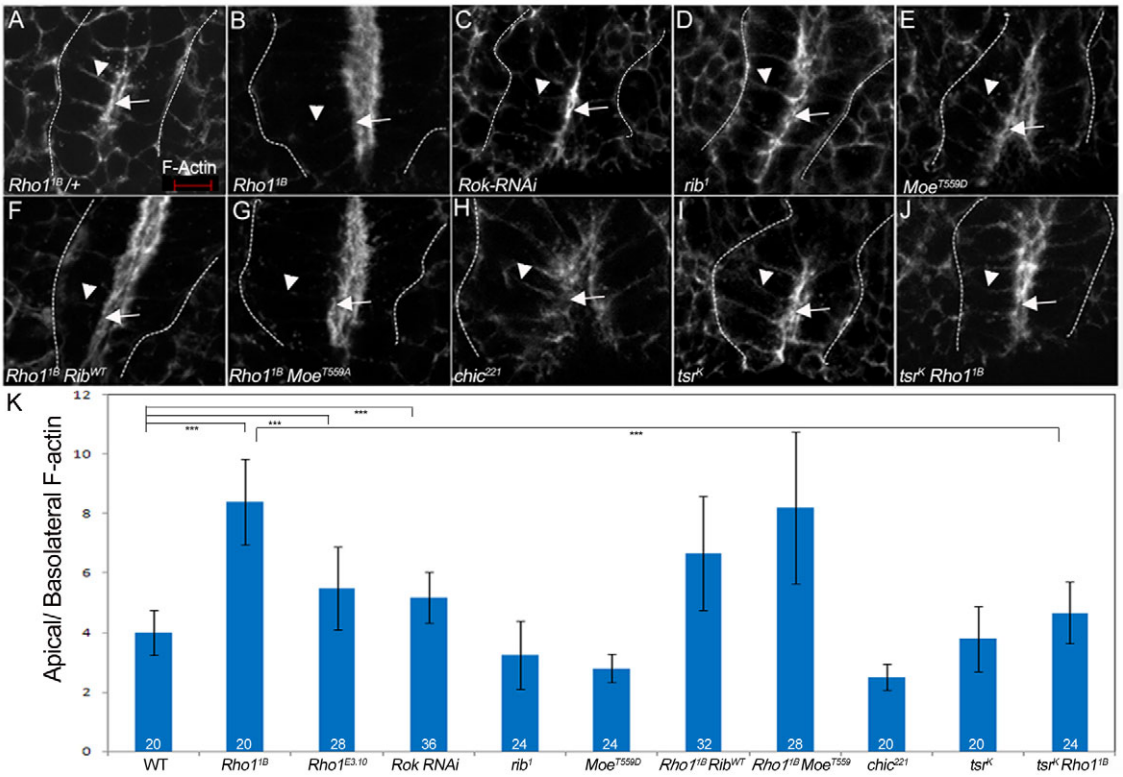

Fig. 4. Rho1 regulates actin polymerization and distribution in salivary gland cells. (**A**) In $Rho1^{1B}$ heterozygous *Drosophila* embryos, F-actin is slightly enriched in the apical membrane (arrow) and is localized along the basolateral membrane (arrowhead). (**B**) In $Rho1^{1B}$ homozygous embryos, F-actin is highly enriched in the apical membrane (arrow) and is reduced from the basolateral membrane (arrowhead). (**C**) In *Rok-RNAi*-expressing glands, F-actin is enriched in the apical membrane (arrow) and reduced from the basolateral membrane (arrowhead). (**D**,**E**) In rib^1 homozygous embryos (D) and wild-type embryos expressing Moe^{T559D} in the gland (E), F-actin is slightly enriched in the apical membrane (arrows) and is present along the basolateral membrane (arrowheads). (**F**,**G**) In $Rho1^{1B}$ homozygous embryos expressing Rib^{WT} (F) or Moe^{T559A} (G), F-actin is highly enriched in the apical membrane (arrows) and is reduced from the basolateral membrane (arrowheads). (**H**) In $chic^{221}$ homozygous embryos, F-actin is disorganized at the apical membrane (arrow) and is present at the basolateral membrane (arrowhead). (**I**,**J**) In tsr^K homozygous embryos (I) and $tsr^K Rho1^{1B}$ double mutant embryos (J), F-actin is slightly enriched in the apical membrane (arrows) and is present along the basolateral membrane (arrowheads). (**K**) Graph depicting the ratio of F-actin at the apical and basolateral membranes in wild-type (WT) glands, glands of $Rho1^{1B}$, $Rho1^{E3.10}$, rib^1, $chic^{221}$, tsr^k, $tsr^k Rho1^{1B}$ homozygous embryos, glands expressing Moe^{T559D} or *Rok-RNAi* and glands of $Rho1^{1B}$ homozygous embryos expressing Rib^{WT} or Moe^{T559A}. Numbers on bars represent the number of cells measured. ***P<0.001. Error bars represent s.d. All embryos shown are at stage 12 and were stained for F-actin with phalloidin. Dashed lines in A-J outline the salivary gland. Scale bar: 5 μm.

shown); however, F-actin distribution between the apical and basolateral membranes was not as severely disrupted as in *Rho1^{1B}* mutant glands (Fig. 4K). Thus, Rho1 and Rok promote F-actin localization at the basolateral membrane and limit F-actin at the apical membrane in salivary gland cells.

Because lumen size defects in *Rho1^{1B}* mutant gland cells were accompanied by a reduction in basolateral F-actin, we hypothesized that promoting actin polymerization by preventing actin depolymerization might restore basolateral F-actin in *Rho1* mutant gland cells. *Twinstar* encodes the only *Drosophila* homolog of Cofilin (Chen et al., 2001), an actin-binding protein, actin-depolymerizing activity of which is inhibited through phosphorylation by LIM-kinase, which, in turn, is regulated by ROCK/Rok (Maekawa et al., 1999). Mutations in *tsr* have been shown to affect border cell migration and planar cell polarity in *Drosophila* (Blair et al., 2006; Zhang et al., 2011). To inhibit *tsr* function in *Rho1^{1B}* salivary gland cells, we used a *tsr* allele, *tsr^{k05633}* (referred to here as *tsr^{k}*) that was shown previously to have no effect on salivary gland development on its own (Chandrasekaran and Beckendorf, 2005). Loss of *tsr* function in *Rho1^{1B}* homozygous embryos significantly suppressed the cell rearrangement and apical domain elongation defects of *Rho1^{1B}* mutant glands, which, in turn, narrowed the expanded lumens (Fig. 3B,D,E). Loss of *tsr* in *Rho1^{1B}* mutant glands had no effect on cell shape change or lumen length (Fig. 3A,C). Salivary glands mutant for *tsr^{k}* alone showed no defect in lumen size or apical domain elongation (data not shown) or F-actin distribution (Fig. 4I,K). In *tsr^{k} Rho1^{1B}* double mutant salivary gland cells, F-actin was distributed normally and localized to the basolateral membrane (Fig. 4J,K). These data suggest that Rho1-mediated regulation of actin polymerization and distribution promotes cell rearrangement and apical domain elongation.

To test whether independent inhibition of actin polymerization can phenocopy the *Rho1* lumen phenotype, we analyzed embryos mutant for *chickadee* (*chic*), encoding the *Drosophila* homolog of profilin, an actin-binding protein that promotes actin polymerization (Cooley et al., 1992). Loss of *chic* disrupts actin-dependent processes during *Drosophila* oogenesis and embryogenesis (Cooley et al., 1992; Verheyen and Cooley, 1994), and overexpression of *chic* in the salivary gland perturbs gland invagination and morphology (Maybeck and Roper, 2009). In *chic^{221}* mutant embryos, gland lumens were widened and shortened, and gland cells failed to elongate their apical domains and rearrange, as was also observed in *Rho1^{1B}* mutant embryos (supplementary material Fig. S6). In contrast to *Rho1^{1B}* mutant

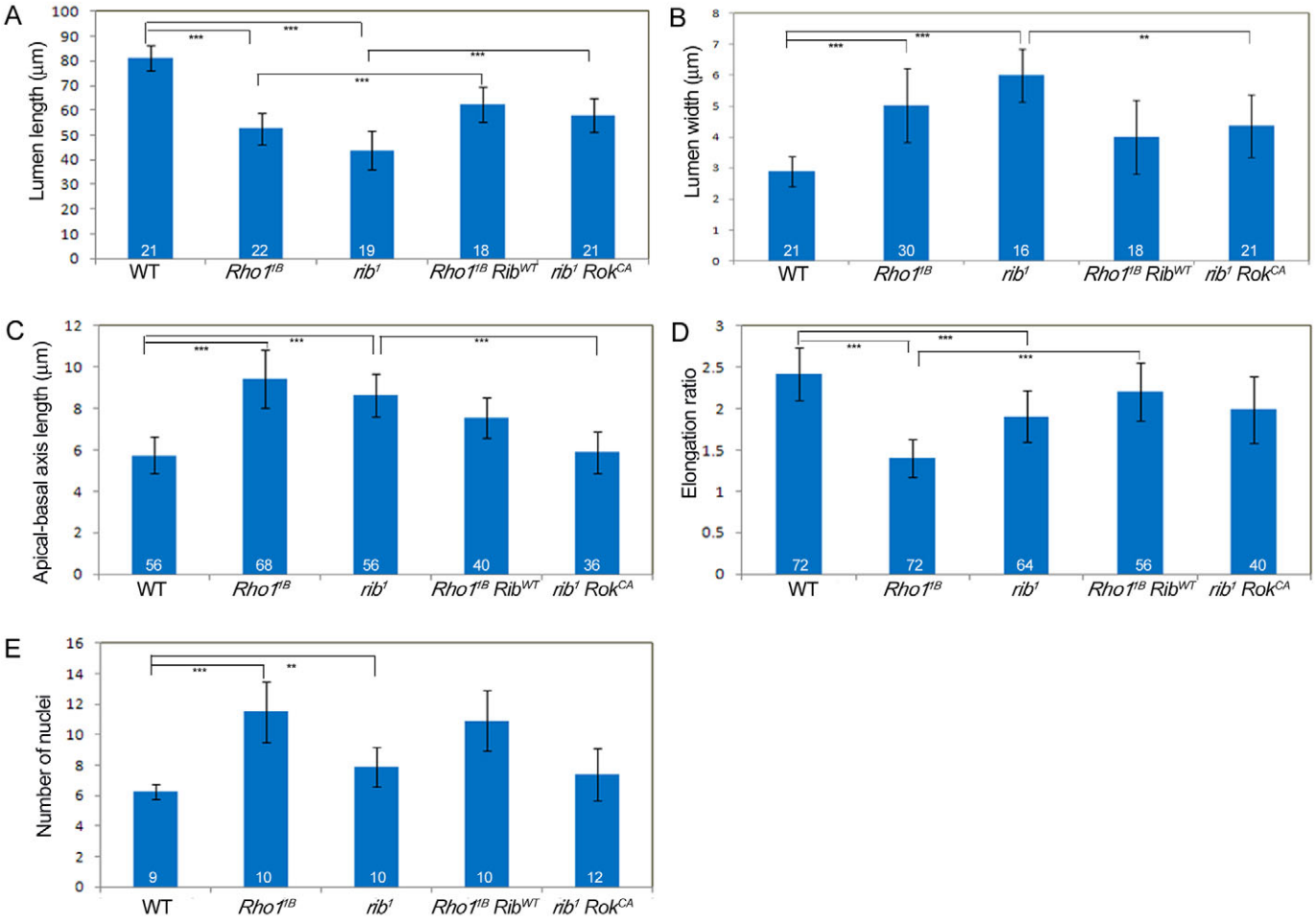

Fig. 5. Ribbon controls salivary gland lumen size. (**A-E**) Graphs depicting measurements of lumen length (A) and width (B), apical-basal axis length (C), apical domain elongation ratio (D) and number of nuclei surrounding the gland lumen (E) in wild-type (WT) *Drosophila* embryos, *Rho1^{1B}* and *rib^{1}* homozygous embryos, *Rho1^{1B}* mutant embryos expressing *Rib^{WT}* in the gland and *rib^{1}* mutant embryos expressing *Rok^{CA}* in the gland. $^{**}P<0.01$, $^{***}P<0.001$. Numbers on bars represent the number of glands (A,B,E) or the number of gland cells (C,D) measured. Error bars represent s.d.

glands, in *chic* mutant glands, F-actin was present at the basolateral membrane and was disorganized at the apical membrane, resulting in an apical-basolateral F-actin ratio lower than that of wild-type glands (Fig. 4H,K). These data suggest that not only is Rho1 required for actin polymerization, but it is also required for the proper distribution of F-actin.

Rho1 controls gland lumen size with Ribbon

The salivary gland lumen size defects of *Rho1* mutant embryos are similar to those of embryos mutant for *ribbon* (*rib*), which encodes a BTB domain transcription factor that is required for the development of multiple epithelial-based tubular organs, such as the salivary gland, Malpighian tubules and trachea (Blake et al., 1999; Bradley and Andrew, 2001; Jack and Myette, 1997; Kerman et al., 2008; Shim et al., 2001) and that is known to control gland lumen size (Kerman et al., 2008). Rib has been proposed to regulate gland lumen size by promoting Crb expression to facilitate apical membrane growth and by limiting apical Moesin activity, which is thought to reduce apical membrane stiffness (Kerman et al., 2008; Cheshire et al., 2008). The rib^{1} allele encodes a truncated Rib protein lacking the C-terminal half owing to a nonsense codon after residue 282 (Bradley and Andrew, 2001). Lumens of rib^{1} mutant glands were shortened and widened to the same severity as those of $Rho1^{1B}$ mutant glands (Fig. 5A,B). rib^{1} mutant gland cells failed to change shape and their apical domains failed to elongate; however, cell rearrangement was only mildly affected (Fig. 5C-E). Moreover, apical and basolateral E-cad levels in rib^{1} mutant glands were comparable to that in heterozygous glands (supplementary material Fig. S2), suggesting that, like Rho1, Rib controls gland lumen size independently of E-cad levels. Expression of wild-type *Rib* (Rib^{WT}) in salivary glands of $Rho1^{1B}$ mutant glands completely suppressed the apical domain elongation defect but had little or no effect on cell rearrangement, cell shape change and lumen size (Fig. 5A-E). Expression of Rok^{CA} in rib^{1} mutant embryos had no effect on apical domain elongation; however, Rok^{CA} did partially restore normal lumen width in rib^{1} mutant glands possibly owing to the effect of Rok^{CA} on cell shape change (Fig. 5B,C). These data suggest that Rib contributes mainly to Rho1-dependent apical domain elongation and not to cell rearrangement.

Rho1 limits apical phosphorylated Moesin

Rib has been shown to regulate apical domain remodeling in gland cells by limiting apical Moesin (Moe) activity (Kerman et al., 2008). In *rib* mutant embryos, levels of phosphorylated Moe (p-Moe), the active form of Moe, were elevated in the apical membrane (Fig. 6C) (Kerman et al., 2008). $Rho1^{1B}$ mutant glands showed highly elevated levels of apical p-Moe, even higher than that of rib^{1} mutant glands (Fig. 6A-C,F,G). $Rho1^{E3.10}$ mutant glands showed a modest but statistically significant accumulation of p-Moe at the apical membrane (Fig. 6G). To test for a role for Moe in salivary gland lumen size control, we analyzed the effects of expressing a non-phosphorylatable form of Moe (Moe^{T559A}), in which the conserved Threonine at 559 is changed to an Alanine (T559A), or a phosphomimetic form of Moe (Moe^{T559D}), in which the conserved Threonine is changed to an Aspartic Acid (T559D) and has been shown to act in a constitutively active manner (Speck et al., 2003). Expression of Moe^{T559A} in $Rho1^{1B}$ mutant glands completely suppressed the apical domain elongation defect (Fig. 7D) but had no effect on the cell rearrangement defect (Fig. 7E), suggesting that the phosphorylated state of Moe at Thr 559 is important for Rho1 regulation of Moe and its effect on apical domain elongation specifically. Expression of Moe^{T559A} alone in wild-type glands did not have any effect on gland lumen size (data not shown). However, expression of Moe^{T559D} completely phenocopied loss of *Rho1*; in Moe^{T559D}-expressing salivary glands, lumens were shorter and wider, cells failed to change shape, apical

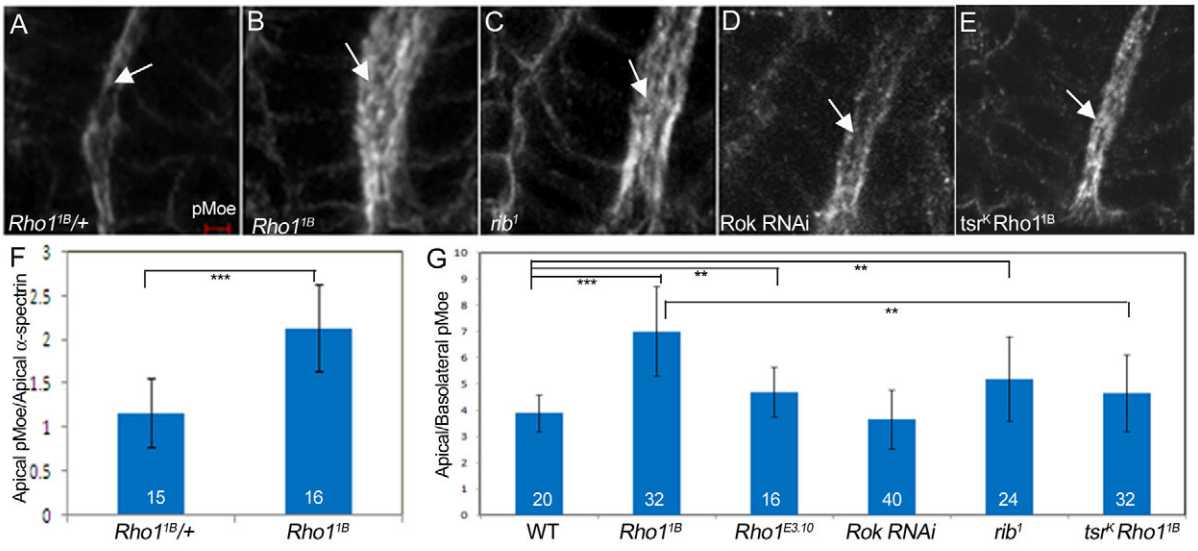

Fig. 6. Rho1 and Ribbon limit apical phosphorylated Moesin in salivary gland cells. (**A-E**) In wild-type *Drosophila* embryos (A), phosphorylated Moesin (p-Moe) is slightly enriched in the apical domain (A, arrow), whereas in $Rho1^{1B}$ (B) and rib^{1} (C) mutant gland cells, it is highly enriched in the apical domain (B and C, arrows). In *Rok-RNAi*-expressing gland cells (D) and $tsr^{K}Rho1^{1B}$ double mutant gland cells (E), p-Moe is slightly enriched in the apical domains (D and E, arrows). All embryos shown are at stage 12. Embryos in A and B were stained for p-Moe and α-spectrin (not shown), whereas embryos in C-E were stained for p-Moe. Scale bar: 2 μm. (**F**) Graph depicting ratio of fluorescence intensity of apical p-Moe to α-spectrin in the proximal gland cells of $Rho1^{1B}$ heterozygous and homozygous embryos. (**G**) Graph depicting ratio of apical to basolateral p-Moe in wild-type, $Rho1^{1B}$, $Rho1^{E3.10}$, *Rok-RNAi*, rib^{1} and $tsr^{K}Rho1^{1B}$ mutant proximal gland cells. $^{**}P<0.01$; $^{***}P<0.001$. Numbers on bars represent the number of gland cells measured. Error bars represent s.d.

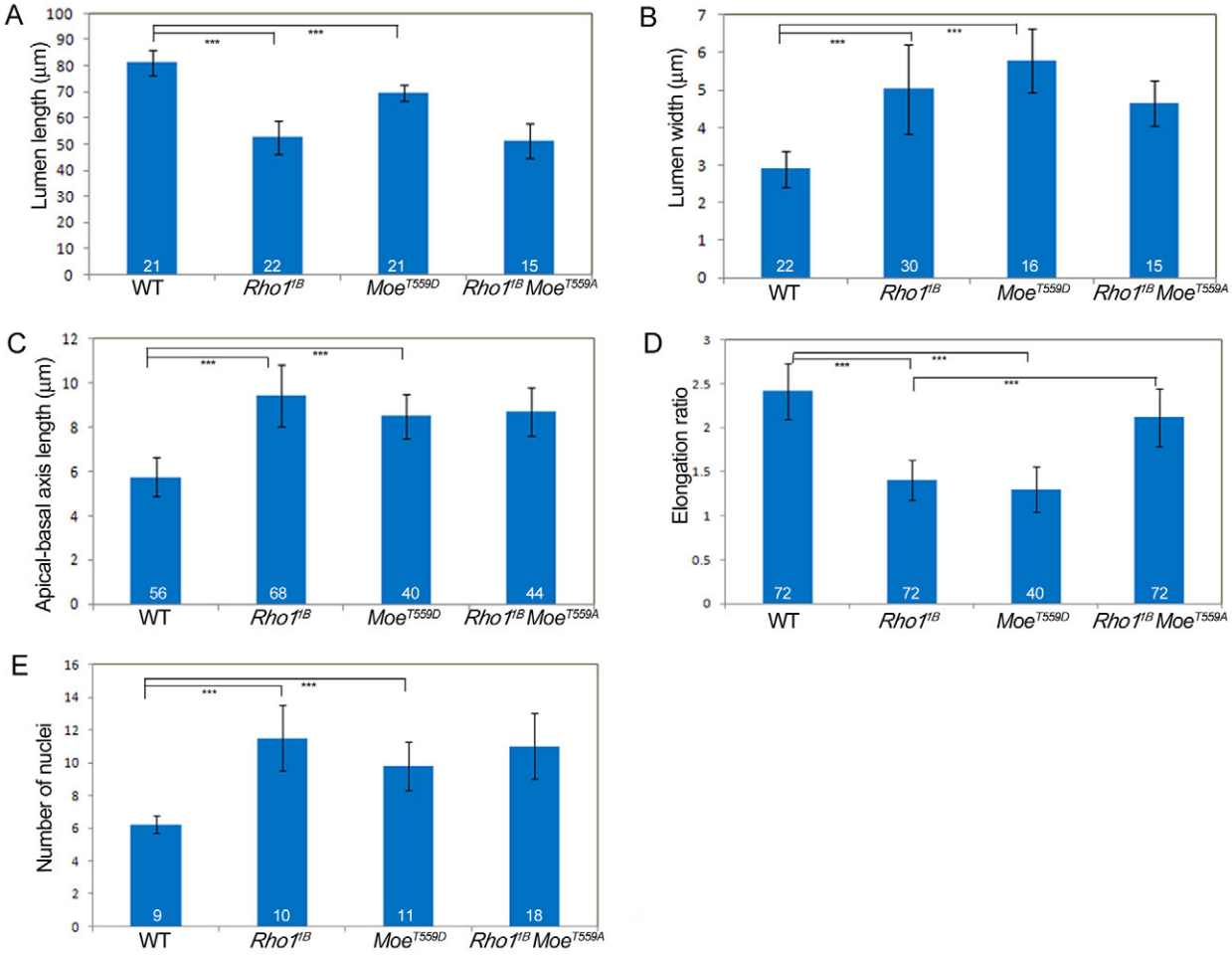

Fig. 7. Regulation of salivary gland lumen size by phosphorylated Moesin. (**A-E**) Graphs depicting measurements of lumen length (A) and width (B), apical-basal axis length (C), elongation ratio of apical domain (D) and number of nuclei surrounding gland lumens (E) in wild-type (WT) *Drosophila* glands, $Rho1^{1B}$ mutant glands, glands expressing Moe^{T559D} and $Rho1^{1B}$ mutant glands expressing Moe^{T559A}. ***P<0.001. Numbers on bars represent the number of glands (A,B,E) or number of gland cells (C,D) measured. Error bars represent s.d.

domains failed to elongate and an increased number of nuclei surrounded the lumen (Fig. 7A-E). Similar to these data, it was previously reported that expression of Moe^{T559A}in *rib* mutant trachea partially suppresses the tracheal defects and overexpression of Moe^{T559D} phenocopies the *rib* mutant phenotype in the gland and trachea (Kerman et al., 2008). In contrast to Rho1, Rok was not required for limiting apical p-Moe; in *Rok-RNAi*-expressing salivary gland cells, p-Moe was not enriched apically (Fig. 6D,G). From these data we conclude that Rho1, independent of Rok, limits apical p-Moe and that this function of Rho1 is important for apical domain elongation but not for cell rearrangement.

In contrast to *Rho1* mutant salivary gland cells, rib^1 mutant gland cells and gland cells expressing Moe^{T559D} showed a normal distribution of F-actin between the apical and basolateral membranes (Fig. 4D,E,K). Expression of either Moe^{T559A} or Rib^{WT} in $Rho1^{1B}$ mutant glands did not alter the apical enrichment of F-actin nor did it restore basolateral F-actin in $Rho1^{1B}$ mutant gland cells (Fig. 4F,G,K). In *tsr* $^{k}Rho1^{1B}$ double mutant embryos, in which loss of *tsr* rescued the cell rearrangement and apical domain elongation defects of $Rho1^{1B}$ mutant glands through proper distribution of F-actin, apical p-Moe was significantly reduced compared with $Rho1^{1B}$ mutant glands (Fig. 6B,E,G). From these data we conclude that the enriched apical F-actin observed in $Rho1^{1B}$ mutant gland cells is not due to the enriched apical p-Moe and that although Rib functions with Rho1 to limit p-Moe, Rib has no effect on F-actin distribution.

Rab5- and Dynamin-mediated endocytosis and actin distribution

We previously showed that Rab5-mediated endocytosis regulates differential localization of E-cad during apical domain elongation in salivary gland cells (Pirraglia et al., 2010). To test whether Rab5-dependent endocytosis plays a role in Rho1-mediated regulation of apical F-actin and/or p-Moe, we first determined whether loss of *Rho1* affected the subcellular distribution of endocytic vesicles. In $Rho1^{1B}$ heterozygous gland cells, F-actin and Avalanche (Aval), a *Drosophila* syntaxin that labels early endosomes (Lu and Bilder, 2005), colocalized at the sub-apical membrane and in intracellular puncta (Fig. 8A). By contrast, in $Rho1^{1B}$ homozygous embryos, Aval and F-actin colocalized at the apical membrane but not in intracellular puncta that lacked F-actin (Fig. 8B). We next tested whether independently inhibiting Rab5- and/or Dynamin-mediated endocytosis phenocopies the *Rho1* gland lumen size defects. Gland-specific expression of

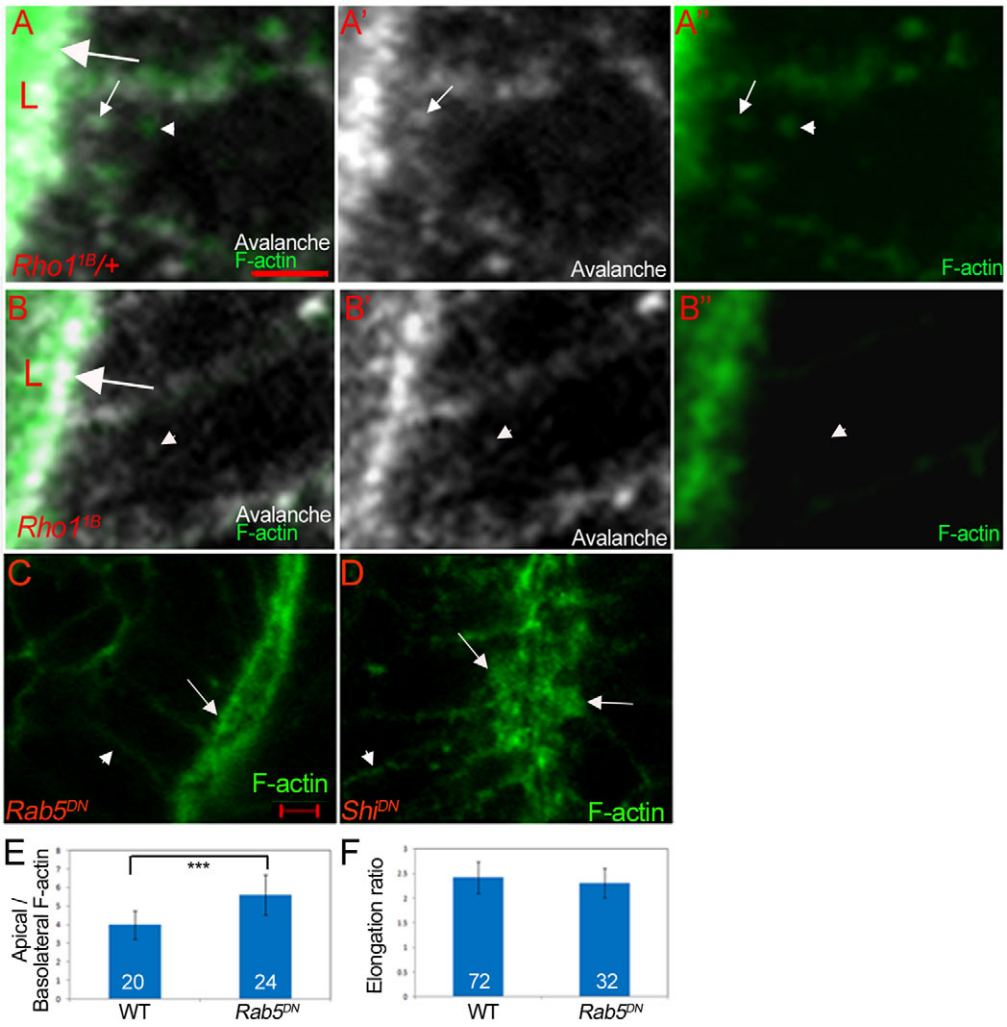

Fig. 8. Rab5 and Dynamin inhibition affects apical F-actin in salivary gland cells. (**A-A″**) In salivary gland cells of *Rho1*^{1B} heterozygous embryos, Avalanche (A and A′, white) and F-actin (A and A″, green) colocalize at the sub-apical membrane (A, large arrow) and in some intracellular puncta (A, small arrow) but not in others (A, arrowhead). (**B-B″**) In *Rho1*^{1B} homozygous embryos, Avalanche (B and B′, white) and F-actin (B and B″, green) colocalize at the sub-apical membrane (B, large arrow) and not in intracellular puncta (B, arrowhead). (**C**,**D**) In gland cells expressing *Rab5*^{DN} (C), F-actin is enriched at the apical membrane (C, arrow) and is present in the basolateral membrane (C, arrowhead), whereas in cells expressing *Shi*^{DN} (D) F-actin is enriched in the apical and sub-apical domains (D, arrows) and is present in the basolateral membrane (D, arrowhead). (**E**) Graph depicting *Rab5*^{DN}-expressing salivary gland cells have higher apical to basolateral F-actin ratio compared with wild-type gland cells. (**F**) Graph depicting *Rab5*^{DN}-expressing gland cells elongated their apical domains to the same extent as wild-type (WT) cells. ***P<0.001. Numbers on bars represent the number of cells measured. Error bars represent s.d. All embryos shown are at stage 12. Embryos in A and B were stained for F-actin with phalloidin (green) and Avalanche (white) to detect early endosomes, whereas embryos in C and D were stained for F-actin. Scale bars: 2 μm.

dominant negative Rab5 (Rab5^{DN}) led to a moderate enrichment of F-actin at the apical membrane although F-actin continued to be localized at the basolateral membrane (Fig. 8C,E). Gland-specific expression of dominant negative *shibire* (*shi*), encoding *Drosophila* Dynamin, (Shi^{DN}), resulted in the dramatic accumulation of F-actin at the apical and sub-apical membrane (Fig. 8D). Although F-actin accumulated apically in *Rab5*^{DN}- or *Shi*^{DN}-expressing gland cells, basolateral F-actin and apical p-Moe were not affected (Fig. 8C,D; data not shown). Apical domain elongation and gland lumen size were also not affected in *Shi*^{DN}- and *Rab5*^{DN}-expressing glands (Fig. 8F; supplementary material Fig. S7). Continued expression of *Shi*^{DN} in the gland resulted in Aval-positive structures coated with F-actin that appeared tethered to the apical membrane (supplementary material Fig. S8). Thus, loss of *Rho1* resulted in loss of F-actin from early endosomes, and inhibition of Rab5 or Shi led to apical enrichment of F-actin but did not affect gland lumen size.

DISCUSSION

We previously showed that Rho1 acts both in salivary gland cells and in the surrounding mesoderm to maintain apical polarity during gland invagination and to mediate cell shape change during gland migration (Xu et al., 2008). Here, we demonstrate a novel role for Rho1 in controlling salivary gland lumen size through regulation of actin polymerization and distribution and regulation of Moesin activity. By analyzing Rho1 alleles for which salivary gland cells invaginated and formed a gland, we showed that zygotic loss of function of Rho1 resulted in shortening and widening of the gland

lumen, which was accompanied by defects in cell shape change and cell rearrangement and failure of apical domains to elongate along the Pr-Di axis of the gland. These effects of Rho1 are mediated through Rok, as inhibition of Rok completely phenocopied loss of Rho1 in these cellular events. Based on these studies, we propose a model for Rho1 control of salivary gland lumen size, in particular lumen width, which is determined by cell rearrangement and apical domain elongation. Rho1 and Rok, through inhibition of cofilin, regulate cell rearrangement and apical domain elongation by promoting actin polymerization to localize F-actin at the basolateral membrane and by limiting the apical accumulation of F-actin (Fig. 9). In parallel to its role in actin polymerization and distribution, Rho1 acts independently of Rok to limit apical p-Moe with Rib by an unknown mechanism and this function of Rho1 is specific for apical domain elongation (Fig. 9). Our data on cofilin are consistent with those in cultured HeLa cells that showed that mammalian ROCK can inhibit cofilin activity indirectly through LIMK-mediated phosphorylation of cofilin (Maekawa et al., 1999).

Although manipulating Moe activity through gland-specific expression of Moe^{T559D} was sufficient to completely phenocopy the *Rho1* lumen defects, including cell rearrangement, it did so without disrupting actin polymerization or distribution. This is likely to be due to activated Moe strengthening the link between the actin cytoskeleton and the apical plasma membrane (without affecting levels of apical F-actin), which would increase apical membrane stiffness and remove the ability of gland cells to rearrange. Indeed, Moesin has been shown to control cortical rigidity during mitosis of cultured *Drosophila* S2R+ cells (Kunda et al., 2008). Thus, Rho1 regulates cell rearrangement and apical domain elongation by controlling the actin cytoskeleton and Moesin activity through distinct mechanisms.

Our observation that *chic* mutant glands phenocopied *Rho1* mutant glands to a large extent, suggests that Rho1 control of salivary gland lumen size is mainly dependent on a requirement for Rho1 in actin polymerization. However, as the *chic* and *Rho1* gland lumen phenotypes are not identical, with *chic* mutant glands lacking the apical accumulation of F-actin and p-Moe observed in *Rho1* mutant glands, Rho1 probably has an additional function in limiting accumulation of F-actin and p-Moe at the apical membrane. This function of Rho1, at least for limiting apical F-actin, might partly involve Rab5- or Shi-mediated endosome trafficking, because inhibition of Rab5 alone or Shi alone led to accumulation of F-actin at the apical membrane. Although $Rab5^{DN}$- or Shi^{DN}-expressing salivary gland cells were enriched with apical F-actin, lumen size was not affected. This could be due to $Rab5^{DN}$ and Shi^{DN} affecting a pool of apical F-actin distinct from that affected by Rho1 and/or because $Rab5^{DN}$-expressing gland cells retain basolateral F-actin and the ratio of apical to basolateral F-actin is not altered sufficiently to cause lumen size defects. In $Rho1^{1B}$ mutant gland cells, some early endosomes were not coated with F-actin. Actin is known to contribute to multiple steps of the endocytic pathway, including movement of endocytic vesicles through the cytoplasm and their transport to late endosomes and lysosomes (Apodaca, 2001; Brown and Song, 2001; Merrifield et al., 1999; Qualmann and Kessels, 2002; Taunton et al., 2000; van Deurs et al., 1995). One possible mechanism by which Rho1 normally limits apical accumulation of F-actin is by promoting its removal from the apical membrane and accumulation on endocytic vesicles.

Currently, we do not know how Rho1 limits accumulation of apical p-Moe. Membrane localization and activity of Moesin can be regulated via a number of mechanisms, such as its phosphorylation on a conserved Threonine residue (Matsui et al., 1998; Ohshiro et al., 1988), binding to phosphatidylinositol-(4,5)bisphosphate [PtdIns(4,5)P2] (Roch et al., 2010; Yonemura et al., 2002) and association with components of the sub-membrane cytoskeleton, such as Crb (Medina et al., 2002). Studies in cultured mammalian cells have demonstrated that Rho signaling activates Moe either through phosphorylation of Moe by ROCK (Matsui et al., 1998) or through ROCK-mediated inhibition of myosin phosphatase, which is known to dephosphorylate p-Moe (Fukata et al., 1998). Although it is possible that *Drosophila* Rho1 positively regulates Moe activity by one or more of these mechanisms, we show here that in the developing salivary glands Rho1 in fact negatively regulates Moe activity. In *rib* mutant embryos, in which p-Moe is enriched apically, salivary gland and tracheal cells showed decreased staining for Rab11 GTPase, which localizes to the apical recycling endosomes and to secretory vesicles destined for the apical membrane (Kerman et al., 2008). Thus, Rho1, like Rib might limit apical p-Moe through its membrane transport.

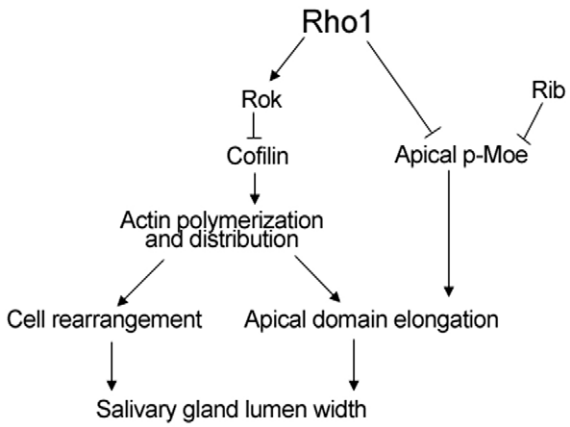

Fig. 9. Model for Rho1-mediated control of salivary gland lumen width. In wild-type embryos, Rho1 promotes actin polymerization and distribution through Rok-mediated inhibition of Cofilin to control salivary gland lumen width by regulating cell rearrangement and apical domain elongation. In parallel, Rho1 acts with Ribbon to promote apical domain elongation by limiting apical phosphorylated Moesin.

In *Drosophila* imaginal disc epithelia, Moe negatively regulates Rho1 activity to maintain epithelial integrity and to promote cell survival (Hipfner et al., 2004; Molnar and de Celis, 2006; Neisch et al., 2010; Speck et al., 2003). Our studies demonstrating that in the developing salivary gland Rho1 antagonizes Moe activity by limiting its localization at the apical membrane, shed novel insight into the functional relationship between Rho1 and Moe. It is possible that in a dynamic epithelium, such as the developing salivary gland, Rho1 contributes to the precise spatial and temporal regulation of Moe activity to fine-tune selective changes in apical domain shape. By contrast, in the imaginal disc epithelium, Rho1 regulation of Moe might not be necessary and, instead, Moe regulation of Rho1 activity is required to maintain epithelial integrity and cell survival. Thus, Rho and Moe can antagonize each other's activities depending on the type of epithelia or cellular event.

Our rescue studies with $Rho1^{WT}$ demonstrated that Rho1 functions predominantly in the salivary gland cells to control apical domain elongation and cell rearrangement. Interestingly, expression of $Rho1^{WT}$ in the mesoderm with *twi*-GAL4 had no effect on cell rearrangement and had little effect on apical

domain elongation and lumen size (this study), whereas we previously showed that $Rho1^{WT}$ expression in the mesoderm significantly rescued the gland migration defect of $Rho1^{1B}$ mutant embryos (Xu et al., 2008). This suggests that gland migration and lumen size control are regulated by distinct mechanisms. In support of this conclusion, embryos mutant for *multiple edematous wings*, encoding the αPS1 integrin subunit, which was previously reported to have defects in gland migration (Bradley et al., 2003), showed no defects in gland lumen width (C. Pirraglia, J. Walters, N. Ahn, M.M.M., unpublished). Identifying the distinct and overlapping mechanisms by which salivary gland lumen width and length are controlled will help to elucidate the mechanisms by which lumen size is controlled in tubular organs.

Acknowledgements
We would like to thank the many generous members of the fly community, the Bloomington Stock Center, Vienna *Drosophila* RNAi Center and the Developmental Studies Hybridoma Bank for providing fly lines and antisera. We acknowledge members of the Myat laboratory for their support and valuable discussions of this work. We are grateful to Deborah Andrew, Alan Hall and Markus Schober for their insightful comments and critical reading of the manuscript. We thank the Rockefeller University Bioimaging Resource Center and the Optical Core Facility at Weill Medical College of Cornell University.

Funding
This work was supported by a Research Scholar Grant (RSG) from the American Cancer Society [to M.M.M.]; and the National Institutes of Health [GM082996 to M.M.M.]. Deposited in PMC for release after 12 months.

Competing interests statement
The authors declare no competing financial interests.

Supplementary material
Supplementary material available online at
http://dev.biologists.org/lookup/suppl/doi:10.1242/dev.069831/-/DC1

References
Andrew, D. and Ewald, A. (2010). Morphogenesis of epithelial tubes: insights into tube formation, elongation and elaboration. *Dev. Biol.* **341**, 34-55.
Apodaca, G. (2001). Endocytic traffic in polarized epithelial cells: role of the actin and microtubule cytoskeleton. *Traffic* **2**, 149-159.
Blair, A., Tomlinson, A., Pham, H., Gunsalus, K., Goldberg, M. and Laski, F. (2006). Twinstar, the Drosophila homolog of cofilin/ADF, is required for planar cell polarity patterning. *Development* **133**, 1789-1797.
Blake, K., Myette, G. and Jack, J. (1999). Ribbon, raw and zipper have distinct functions in reshaping the *Drosophila* cytoskeleton. *Dev. Genes Evol.* **9**, 555-559.
Bradley, P. B. and Andrew, D. J. (2001). Ribbon encodes a novel BTB/POZ protein required for directed cell migration in *Drosophila melanogaster. Development* **128**, 3001-3015.
Bradley, P. L., Myat, M. M., Comeaux, C. A. and Andrew, D. J. (2003). Posterior migration of the salivary gland requires an intact visceral mesoderm and integrin function. *Dev. Biol.* **257**, 249-262.
Brown, B. and Song, W. (2001). The actin cytoskeleton is required for the trafficking of the b cell antigen receptor to the late endosomes.. *Traffic* **2**, 414-427.
Chandrasekaran, V. and Beckendorf, S. (2005). Tec29 controls actin remodeling and endoreplication during invagination of the *Drosophila* embryonic salivary glands. *Development*, 3515-3524.
Chen, J., Godt, D., Gunsalus, K., Kiss, I., Goldberg, M. and Laski, F. (2001). Cofilin/ADF is required for cell motility during Drosophila ovary development and oogensis. *Nat. Cell Biol.* **3**, 204-209.
Cheshire, A., Kerman, B., Zipfel, W., Spector, A. and Andrew, D. (2008). Kinetic and mechanical analysis of live tube morphogenesis. *Dev. Dyn.* ***237***, 2874-2888.
Cooley, L., Verheyen, E. and Ayers, K. (1992). chickadee encodes a profilin required for intercellular cytoplasm transport during Drosophila oogenesis. *Cell* **69**, 173-184.
Davis, G., Koh, W. and Stratman, A. (2007). Mechanisms controlling human endothelial lumen formation and tube assembly in three-dimensional extracellular matrices. *Birth Defects Res. C Embryo Today* **81**, 270-285.
Fischer, J., Acosta, S., Kenny, A., Cater, C., Robinson, C. and Hook, J. (2004). Drosophila klarsicht has distinct subcellular localization domains for nuclear envelope and microtubule localization in the eye. *Genetics* **168**, 1385-1393.
Fischer-Vize, J. A. and Mosley, K. L. (1994). Marbles mutants: uncoupling cell determination and nuclear migration in the developing *Drosophila* eye. *Development* **120**, 2609-2618.
Fukata, Y., Kimura, K., Oshiro, N., Saya, H., Matsuura, Y. and Kaibuchi, K. (1998). Association of the myosin-binding subunit of myosin phosphatase and moesin: dual regulation of moesin phosphorylation by Rho-associated kinase and myosin phosphatase. *J. Cell Biol.* **141**, 409-418.
Guo, Y., Jangi, S. and Welte, M. (2005). Organelle-specific control of intracellular transport: distinctly targeted isoforms of the regulator Klar. *Mol. Biol. Cell* **16**, 1406-1416.
Halsell, S., Chu, B. and Kiehart, D. (2000). Genetic analysis demonstrates a direct link between Rho signaling and nonmuscle myosin function during Drosophila morphogenesis. *Genetics* **155**, 1253-1265.
Henderson, K. D. and Andrew, D. J. (2000). Regulation and function of *Scr*, *exd*, and *hth* in the *Drosophila* salivary gland. *Dev. Biol.* **217**, 362-374.
Hipfner, D., Keller, N. and Cohen, S. (2004). Slik Sterile-20 kinase regulates Moesin activity to promote epithelial integrity during tissue growth. *Genes Dev.* **18**, 2243-2248.
Jack, J. and Myette, G. (1997). The genes raw and ribbon are required for proper shape of tubular epithelial tissues in *Drosophila*. *Genetics* **147**, 243-253.
Jaffe, A., Kaji, N., Durgan, J. and Hall, A. (2008). Cdc42 controls spindle orientation to position the apical surface during epithelial morphogenesis. *J. Cell Biol.* **183**, 625-633.
Jani, K. and Schöck, F. (2007). Zasp is required for the assembly of functional integrin adhesion sites. *J. Cell Biol.* **179**, 1583-1597.
Jung, A. C., Denholm, B., Skaer, H. and Affolter, M. (2005). Renal tubule development in Drosophila: a closer look at the cellular level. *J. Am. Soc. Nephrol.* **16**, 322-328.
Kerman, B., Chesire, A., Myat, M. and Andrew, D. (2008). Ribbon modulates apical membrane during tube elongation through Crumbs and Moesin. *Dev. Biol.* **320**, 278-288.
Kesavan, G., Sand, F., Greiner, T., Johansson, J, Kobberup, S., Wu, X., Brakebusch, C. and Semb, H. (2009). Cdc42-mediated tubulogenesis controls cell specification. *Cell* **139**, 791-801.
Kunda, P., Pelling, A., Liu, T. and Baum, B. (2008). Moesin controls cortical rigidity, cell rounding, and spindle morphogenesis during mitosis. *Curr. Biol.* **18**, 91-101.
Lu, H. and Bilder, D. (2005). Endocytic control of epithelial polarity and proliferation in Drosophila. *Nat. Cell Biol.* **7**, 1232-1239.
Lubarsky, B. and Krasnow, M. A. (2003). Tube morphogenesis: making and shaping biological tubes. *Cell* **112**, 19-28.
Maekawa, M., Ishizaki, T., Boku, S., Watanabe, N., Fujita, A., Iwamatsu, A., Obinata, T., Ohashi, K., Mizuno, K. and Narumiya, S. (1999). Signaling from Rho to the actin cytoskeleton through protein kinases ROCk and LIM-kinase. *Science* **285**, 895-898.
Magie, C. and Parkhurst, S. (2005). Rho1 regulates signaling events required for proper Drosohila embryonic development. *Dev. Biol.* **278**, 144-154.
Magie, C., Meyer, M., Gorsuch, M. and Parkhurst, S. (1999). Mutations in the Rho1 small GTPase disrupt morphogenesis and segmentation during early Drosophila development. *Development* **126**, 5353-5364.
Martin-Belmonte, F. and Mostov, K. (2008). Regulation of cell polarity during epithelial morphogenesis. *Curr. Opin. Cell Biol.* **20**, 227-234.
Martin-Belmonte, F., Gassama, A., Datta, A., Yu, W., Rescher, U., Gerke, V. and Mostov, K. (2007). PTEN-mediated apical segregation of phosphoinositides controls epithelial morphogenesis through Cdc42. *Cell* **128**, 383-397.
Matsui, T., Maeda, M., Doi, Y., Yonemura, S., Amano, M., Kaibuchi, K., Tsukita, S. and Tsukita, S. (1998). Rho-kinase phosphorylated COOH-terminal threonines of ezrin/radixin/moesin (ERM) proteins and regulates their head-to-tail association. *J. Cell Biol.* **140**, 647-657.
Maybeck, V. and Roper, K. (2009). A targeted gain-of-function screen identifies genes affecting salivary gland morphogenesis/tubulogenesis in Drosophila. *Genetics* **181**, 543-565.
Medina, E., Williams, J., Klipfell, E., Zarnescu, D., Thomas, G. and Bivic, A. L. (2002). Crumbs interacts with moesin and β Heavy-spectrin in the apical membrane skeleton of *Drosophila*. *J. Cell Biol.* **158**, 941-951.
Merrifield, C., Moss, S., Ballestrem, C., Imhof, B., Giese, G., Wunderlich, I. and Aimers, W. (1999). Endocytic vesicless move at the tips of actin tails in cultured mast cells. *Nat. Cell Biol.* **1**, 72-74.
Molnar, C. and de Celis, J. (2006). Independent roles of Drosophila Moesin in imaginal disc morphogenesis and hedgehog signalling. *Mech. Dev.* **123**, 337-351.
Mosley-Bishop, K. L., Li, Q., Patterson, L. and Fischer, J. A. (1999). Molecular analysis of the *klarsicht* gene and its role in nuclear migration within differentiating cells of the *Drosophila* eye. *Curr. Biol.* **9**, 1211-1220.
Myat, M. M. and Andrew, D. J. (2002). Epithelial tube morphology is determined by the polarized growth and delivery of apical membrane. *Cell* **111**, 879-891.

Neisch, A., Speck, O., Stronach, B. and Fehon, R. (2010). Rho1 regulates apoptosis via activation of the JNK signaling pathway at the plasma membrane. *J. Cell Biol.* **189**, 311-323.
Ohshiro, N., Fukata, Y. and Kaibuchi, K. (1988). Phosphorylation of moesin by rho-associated kinase (Rho-kinase) plays a crucial role in the formation of microvilli-like structures. *J. Biol. Chem.* **273**, 34663-34666.
Pirraglia, C., Walters, J. and Myat, M. M. (2010). Pak1 control of E-cadherin endocytosis regulates salivary gland lumen size and shape. *Development* **137**, 4177-4189.
Qualmann, B. and Kessels, M. (2002). Endocytosis and the cytoskeleton. *Int. Rev. Cytol.* **220**, 93-144.
Rangarajan, R., Gong, Q. and Gaul, U. (1999). Migration and function of glia in the developing *Drosophila* eye. *Development* **126**, 3285-3292.
Reed, R., Womble, M., Dush, M., Tull, R., Bloom, S., Morckel, A., Devlin, E. and Nascone-Yoder, N. (2009). Morphogenesis of the primitive gut tube is generated by Rho/ROCK/myosin II-mediated endoderm rearrangements. *Dev. Dyn.* **238**, 3111-3125.
Reuter, R., Panganiban, G. E. F., Hoffman, F. M. and Scott, M. P. (1990). Homeotic genes regulate the spatial expression of putative growth factors in the visceral mesoderm of *Drosophila* embryos. *Development* **110**, 1031-1040.
Ridley, A. and Hall, A. (1992). The small GTP-binding protein rho regulates the assembly of focal adhesions and actin stress fibers in response to growth factors. *Cell* **70**, 389-399.
Roch, F., Polesello, C., Roubinet, C., Martin, M., Roy, C., Valenti, P., Carreno, S., Mangeat, P. and Payre, F. (2010). Differential roles of PtdIns(4,5)P_2 and phosphorylation in moesin activation during *Drosophila* development. *J. Cell Sci.* **123**, 2058-2067.
Shim, K., Blake, K. J., Jack, J. and Krasnow, M. A. (2001). The *Drosophila* ribbon gene encodes a nuclear BTB domain protein that promotes epithelial migration and morphogenesis. *Development* **128**, 4923-4933.
Simoes, S., Denholm, B., Azevedo, D., Sotillos, S., Martin, P., Skaer, H., Hombria, J. and Jacinto, A. (2006). Compartmentalisation of Rho regulators directs cell invagination during tissue morphogenesis. *Development* **133**, 4257-4267.
Speck, O., Hughes, S. C., Noren, N. K., Kulikauskas, R. M. and Fehon, R. G. (2003b). Moesin functions antagonistically to the Rho pathway to maintain epithelial integrity. *Nature* **421**, 83-87.
Strutt, D., Weber, U. and Mlodzik, M. (1997). The role of RhoA in tissue polarity and Frizzled signalling. *Nature* **387**, 292-295.
Suzuki, N., Buechner, M., Nishiwaki, K., Hall, D. H., Nakanishi, H., Takai, Y., HIsamoto, N. and Matsumoto, K. (2001). A putative GDP-GTP exchange factor is required for development of the excretory cell in *Caenorhabditis elegans*. *EMBO Rep.* **2**, 530-535.
Taunton, J., Rowning, B., Coughlin, M., Wu, M., Moon, R., Mitchison, T. and Larabell, C. (2000). Actin-dependent propulsion of endosomes and lysosomes by recruitment of N-WASP. *J. Cell Biol.* **148**, 519-530.
Tepass, U. and Knust, E. (1993). Crumbs and Stardust act in a genetic pathway that controls the organization of epithelia in *Drosophila melanogaster*. *Dev. Biol.***159**, 311-326.
Tepass, U., Theres, C. and Knust, E. (1990). *crumbs* encodes an EGF-like protein expressed on apical membranes of *Drosophila* epithelial cells and required for organization of epithelia. *Cell* **61**, 787-799.
van Deurs, B., Holm, P., Kayser, L. and Sandvig, K. (1995). Delivery to lysosomes in the human carcinoma cell-line Hep-2 involves an actin filament-facilitated fusion between mature endosomes and preexisting lysosomes. *Eur. J. Cell Biol.* **66**, 309-323.
Verheyen, E. and Cooley, L. (1994). Profilin mutations disrupt multiple actin-dependent processes during Drosophila development. *Development* **120**, 717-728.
Vining, M. S., Bradley, P. L., Comeaux, C. A. and Andrew, D. J. (2005). Organ positioning in *Drosophila* requires complex tissue-tissue interactions. *Dev. Biol.* **287**, 19-34.
Xu, N., Keung, B. and Myat, M. (2008). Rho GTPase controls invagination and cohesive migration of the *Drosophila* salivary gland through Crumbs and Rho-kinase. *Dev. Biol.* **321**, 88-100.
Yonemura, S., Matsui, T., Tsukita, S. and Tsukita, S. (2002). Rho-dependent and -independent activation mechanisms of ezrin/radixin/moesin proteins: an essential role for polyphosphoinositides in vivo. *J. Cell Sci.* **115**, 2569-2580.
Zhang, L., Luo, L., Wan, P., Wu, J., Laski, F. and Chen, J. (2011). Regulation of cofilin phosphorylation and asymmetry in collective cell migration during morphogenesis. *Development* **138**, 455-464.